Fatigue of swollen elastomers

Mei Sze Loo [a], Jean-Benoît Le Cam [b], Andri Andriyana [a,*], Eric Robin [b], Amalina Muhammad Afifi [a]

[a] Department of Mechanical Engineering, Faculty of Engineering, University of Malaya, 50603 Kuala Lumpur, Malaysia
[b] Université de Rennes 1, Institut de Physique de Rennes UMR CNRS 6251, Campus de Beaulieu, Bât. 10B, 35042 Rennes Cedex, France

ARTICLE INFO

Article history:
Received 4 September 2014
Received in revised form 20 November 2014
Accepted 27 November 2014
Available online 15 December 2014

Keywords:
Nitrile rubber
Swollen rubber
Fatigue damage
Crack nucleation
Biodiesel

ABSTRACT

The compatibility of the properties of elastomer with conventional diesel fuel has made it favourable in many engineering applications. However, due to global energy insecurity issues, there is an urgent need to find alternative renewable sources of energy as replacements to conventional diesel. In this respect, biodiesel appears to be a promising candidate. Hence, research into the compatibility and fatigue characteristics of elastomers exposed to biodiesel becomes essential. The present paper introduces the first attempt to investigate the effect of different solvents on the fatigue of swollen elastomers. The filled nitrile rubbers are immersed in the palm biodiesel and conventional diesel to obtain the same degree of swelling prior to the application of uniaxial fatigue loading. Field Emission Scanning Electron Microscopy (FESEM) analysis is carried out to observe the fracture surfaces. Stretch-N curves are plotted to illustrate the fatigue life duration. These curves showed that the fatigue lifetime of rubber is the longest for dry rubber and the least for rubber swollen in biodiesel. FESEM micrographs reveal that the loading conditions have no effect on the crack initiation and propagation patterns regardless of the swelling state.

1. Introduction

Conventional petroleum-derived fuels are no longer seen as a futuristic source of fuel because of their ever increasing cost and the continuous diminution in supply. This condition has driven researchers to intensively explore the prospects of biodiesel as a renewable energy alternative for future substitution of current depleting energy resources [14]. Beside being eco-friendly, biodiesel's technical advantages have attracted the interest of researcher to comprehensively investigate its properties, potentials and applications. In Southeast Asia, countries like Malaysia and Indonesia are amongst the largest palm biodiesel producers in the world. Indeed, the production in these countries becomes even more favourable in view of the existing tropical climate [12,5].

The reported studies also confirm the influence of biodiesel on elastomers seeing that they have been exploited extensively in the sealing and automotive industries. These studies were motivated by the compatibility of elastomers and biodiesel, which remains a major challenge to date [15]. This concern arises especially when elastomeric components start to degrade in terms of mechanical properties even without any simultaneous imposed loading [31,15,2]. Undeniably, the degradation takes place with swelling [3] when biodiesel creates a hostile environment for elastomeric components.

During service, elastomeric components are usually subjected to cyclic loadings for long durations. For instance, vibration isolators, gaskets and seals are a few common components utilized for this condition. Elastomeric components which endure continuous cyclic loadings may experience fatigue failure [7]. Mars and his co-workers utilized the crack nucleation approach in their works [23–25] to investigate and to predict the appearance of a 1 mm fatigue crack length at the surface of rubber. It was explained that fatigue crack nucleation life can be interpreted as the growth period of pre-existing micro-cracks (smaller than 0.1 mm in size) [24].

Later, Le Cam et al. [21,18] affirmed this finding through a detailed description in their research on the mechanism of crack growth from microscopic flaws, which subsequently led to the appearance of macroscopic crack initiation under uniaxial and multiaxial fatigue loading conditions.

So far, investigations carried out into elastomer fatigue mainly focus on dry elastomers. The very few reported works on swollen elastomers under fatigue loading are dedicated to the effect of oil diffusion into elastomers. Cho et al. [11] discussed the variation of fatigue crack growth resistance of elastomer in the swollen state while Jerrams et al. [16] presented the Wöhler curves at failure obtained from equibiaxial loading conditions. No studies are reported for the fatigue of swollen elastomers by palm biodiesel to date.

* Corresponding author. Fax: +60 3 79 67 53 17.
E-mail address: andri.andriyana@um.edu.my (A. Andriyana).

http://dx.doi.org/10.1016/j.ijfatigue.2014.11.015
0142-1123/

The current studies, which deal with the effect of palm biodiesel diffusion on the behaviour of rubbers, investigate the change of mass, volume, hardness and tensile strength of rubbers for different immersion durations [31,15,14,2]. Haseeb et al. [14] had immersed nitrile rubbers in diesel and biodiesel for 1000 h at room temperature prior to subjecting the specimens to tensile tests. They reported lower tensile strength values for the swollen biodiesel rubbers compared with the swollen diesel rubbers. Meanwhile, Alves et al. [2] conducted similar tests for the nitrile rubbers for a 100 h immersion duration. Their investigations contradict the results of Haseeb et al. [14]. In their research, the measured tensile strength values for the swollen biodiesel appeared to be higher. This contradiction highlights the importance of immersion duration which governs the final swollen state of rubber without disregarding other essential factors such as the compounding ingredients and specimen geometry.

The present paper proposes a first approach to investigating the response of elastomers swollen by palm biodiesel under fatigue loading conditions. For comparison, fatigue characteristics of elastomers swollen by conventional Malaysian diesel fuel are also investigated. For this purpose, the rubber specimens were immersed in these two different solvents in order to obtain swollen rubbers having the same degree of swelling. Moreover, the physical fatigue damage mechanism induced by the presence of biodiesel in the material at the macro and the microscale will also be probed.

2. Experimental setup

2.1. Material and specimen geometry

The material used here was of a commercial grade of carbon black-filled nitrile rubber. It was filled with 25 wt% of carbon black and its hardness was 60 shore A. It is denoted as F-NBR in the rest of the paper. Following Chng et al. [10], the rubber specimens used in the study corresponded to a hollow-diabolo having a height, outer diameter, and wall thickness of 55 mm, 25 mm, and 6 mm, respectively. The detailed features of the specimen and chemical compositions of the palm biodiesel (B100) used in he study are provided in Fig. 1 and Table 1.

The swollen rubber specimens were obtained by immersing initially dry F-NBR in conventional diesel (B0) and palm biodiesel (B100) with the assigned immersion durations in Table 2. The percentage of volume change of the swollen rubbers were calculated using the following equation in accordance to the ASTM D471 standard:

$$\Delta V\% = \frac{(M_3 - M_4) - (M_1 - M_2)}{M_1 - M_2} \times 100 \quad (1)$$

where ΔV is the change in volume, M_1 is the initial mass of specimen in air, M_2 is the initial mass of specimen in water, M_3 is the mass of specimen in air after immersion, M_4 is the mass of specimen in water after immersion.

In the following sections, the swelling in rubber specimens is described in terms of the degree of swelling, J_s, defined by the ratio between the volume of swollen specimen and that of a dry specimen. In order to achieve a certain degree of swelling of F-NBR, it is worth noting that the required immersion duration will be different when different solvents are used.

No standard is followed regarding the choice of the specimens and immersion durations. The hardness and mass value of swollen rubbers were measured before and after fatigue testing. Later, the percentage of hardness and mass change were calculated using the following equations to investigate the effect of solvent type on the hardness and on the degree of swelling during the specimens undergoing fatigue testing:

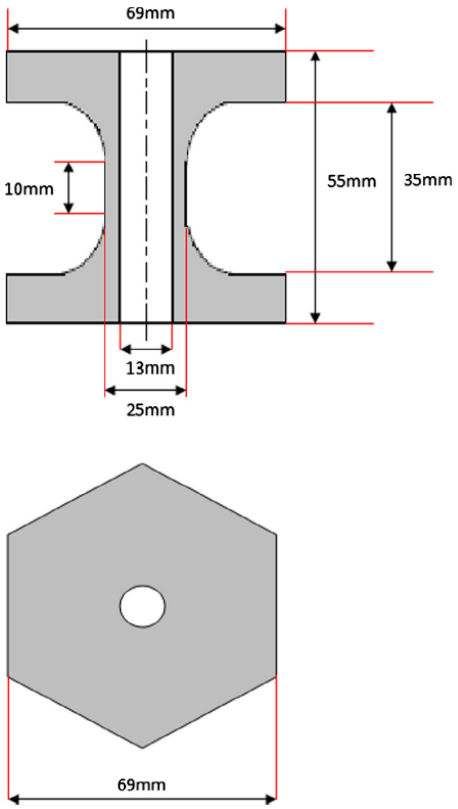

Fig. 1. Geometry of rubber specimen.

Table 1
Properties of B100 palm biodiesel.

Test	% Unit	Methods	Results
Ester content	% (m/m)	EN 14103	96.9
Density at 15 °C	kg/m^3	EN ISO 12185	875.9
Viscosity at 40 °C	mm^2/s	EN ISO 3104	4.667
Flash point	°C	EN ISO 3679	168
Cetane number	–	EN ISO 5165	69.7
Water content	mg/kg	EN ISO 12937	155
Acid value	mgKOH/g	EN ISO 3679	0.38
Methanol content	% (m/m)	EN 14110	<0.01
Monoglyceride content	% (m/m)	EN 14105	0.67
Diglyceride content	% (m/m)	EN 14105	0.2
Triglyceride content	% (m/m)	EN 14105	0.2
Total glycerine	% (m/m)	EN 14105	0.25

$$\Delta H = \frac{H_i - H_s}{H_s} \times 100 \quad (2)$$

$$\Delta M = \frac{M_i - M_s}{M_s} \times 100 \quad (3)$$

where ΔH is the percentage of change in hardness, H_i is the hardness value of the swollen rubber after testing, H_s is the hardness value of the swollen rubber before testing, ΔM is the change in

Table 2
Immersion duration of rubber with their respective solvents.

Rubber	Volume change (%)	Immersion duration	Degree of swelling, J_s
Dry	0	0	1
Swollen B0	5	3 months	1.05
Swollen B100	5	10 days	1.05

mass, M_i is the mass in air of the swollen rubber after testing, M_s is the mass in air of the swollen rubber before testing.

2.2. Loading conditions

2.2.1. Uniaxial cyclic test

The uniaxial cyclic test was performed to investigate the effect of solvents on stress-softening, also referred to as the Mullins effect in the literature [27], for the quasi-static behaviour of swollen rubbers. This investigation is essential since the Mullins effect significantly affects fatigue life [22]. Indeed, under uniaxial fatigue loading conditions, the loss of stiffness in dry elastomers can lead to an increase in fatigue life. It is therefore relevant to characterize the effect of stress-softening on the fatigue life of swollen rubbers. The tests were carried out using an Instron tensile testing machine with a load cell capacity of 10 kN. The rubbers were stretched up to a maximum stretch ratio of 4 for 10 cycles at a 0.1 s^{-1} constant stretch rate. Note that the stretch is defined by the ratio of the stretched length to the initial length of the rubber specimen. In the case of swollen rubbers, the specimen initial length corresponded to the swollen-unstrained length.

2.2.2. Uniaxial fatigue test

The fatigue tests were conducted using a 5 kN Shimadzu 4830 testing machine under prescribed sinusoidal displacement. The load cell capacity used was 5 kN. Fig. 2 portrays an overview of the experimental setup. In the current investigation, R_ϵ was the loading ratio in terms of strain or the nominal strain loading ratio. It is defined as the ratio between the minimum (ϵ_{min}) and the maximum (ϵ_{max}) strain levels applied to the specimen. The loading condition here corresponds to the repeated uniaxial tension, so R_ϵ was equal to zero. The dry and swollen rubbers were subjected to four levels of maximum stretch at room temperature: 1.5, 1.75, 1.9 and 2. The stretch rate of the material lay within the range of 1 $s^{-1} < \dot{\lambda} < 2.5$ s^{-1} such that it would not induce significant thermal effect in the material. The frequency imposed for all loading conditions was 1 Hz except for the maximum stretch of 1.5, where a frequency of 2 Hz was applied. For each test, the number of cycles required for the appearance of 1 mm crack and for specimen complete rupture was recorded. The test was stopped at 2 million cycles if no crack or rupture is observed in the specimen.

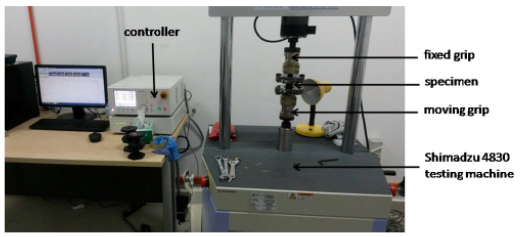

Fig. 2. Overview of experimental setup.

2.3. Field Emission Scanning Electron Microscopy (FESEM)

Specimen surfaces were observed with a Jeol JSM T100F Field Emission Scanning Electron Microscope (FESEM). The Energy Dispersive Spectrometer of X-rays (EDS) coupled with the FESEM were utilized to identify the chemical elements present at the surface of the material. In order to investigate the fracture surfaces, the specimens were previously coated with a thin gold layer by vapour deposition.

3. Results

In this section, the results obtained from the cyclic and fatigue tests are reported for dry and swollen rubbers.

3.1. Hardness and mass change

The measured average hardness values for all specimens before and after fatigue testing are tabulated in Table 3. The values of change of hardness in percentage in the table are calculated using Eq. (2). Table 4 shows the values for mass measurements and the change of mass was calculated using Eq. (3). The negative sign in the percentage shows that there was a decrease of hardness and mass for swollen rubbers. The decrease in hardness for swollen B100 rubber was slightly higher than swollen B0 while the decrease in mass for both is comparable. The decrease in mass for both was less than 0.5% which suggests that the rubber remained swollen throughout the tests with no significant amount of liquid lost. From Table 3, it is observed that the exposure of rubber to solvents leads to a decrease in the hardness. Indeed, before the fatigue tests, the hardness values of dry, swollen B0 and swollen B100 rubbers were 59.5, 54.81 and 54.73 respectively. The corresponding observation could be attributed to the chain scission mechanism [15] and decreased viscosity due to swelling [8]. After undergoing fatigue loading, further decreases in the hardness were observed: 9% in swollen B0 and 11% in swollen B100. It is important to note that this significant change was not observed for the dry rubbers. Hence, this implies that the mechanical loading magnifies the effect of swelling instead of depreciating the hardness of rubber. Since mechanical loading does not induce any additional swelling, the chain scission mechanism seems to be the main reason for the declining values of hardness. This explains the decreasing hardness values from 54.81 and 54.73 (before testing) to 49.84 and 48.62 (after testing) for B0 and B100 respectively.

3.2. Uniaxial cyclic test

The stretch-stress responses of dry and swollen rubbers under cyclic loading are given in Fig. 3a. In general, it is observed that both dry and swollen rubbers show similar inelastic responses. These inelastic responses include stress-softening, hysteresis and permanent set. Similar to the classical softening effect in the dry rubbers, no significant difference of softening was observed from the second cycle onwards for the swollen rubbers. However, it appears that swelling decreased the stress-softening, with a greater decline observed in swollen B0 rubber. At the same time, it was also shown that the stress value was the lowest for the

Table 3
Hardness values of dry and swollen rubbers before and after fatigue tests.

Rubber	Before testing	After testing	Hardness change (−%)
Dry	59.5	59	0.8
Swollen B0	54.81	49.84	9
Swollen B100	54.73	48.62	11

Table 4
Mass of dry and swollen rubbers before and after fatigue test.

Rubber	Before testing (g)	After testing (g)	Mass change (−%)
Dry	127.25	127.24	0
Swollen B0	131.69	131.17	0.39
Swollen B100	131.36	130.86	0.38

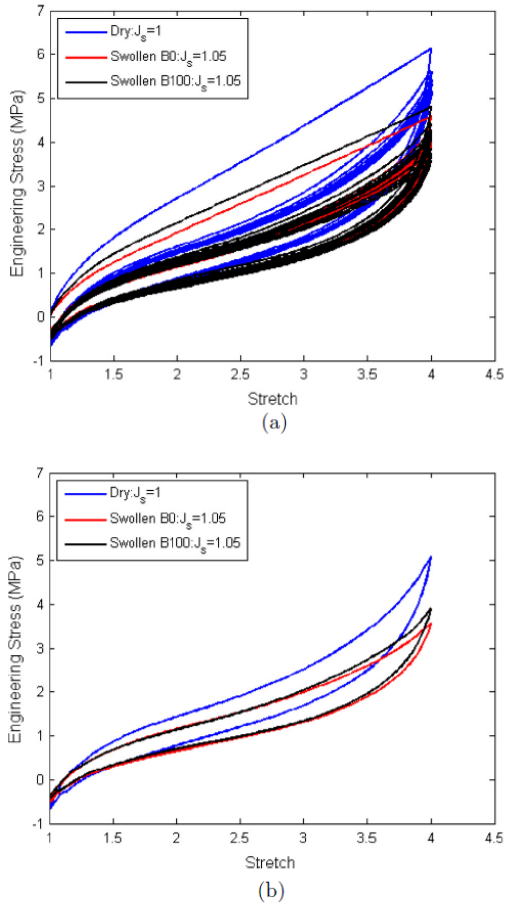

Fig. 3. Stretch-stress response of rubbers under uniaxial cyclic loading. (a) All 10 cycles. (b) At the 10th cycle.

swollen B0 rubber. Fig. 3b illustrates the stretch-stress response of rubbers for the 10th cycle which corresponds to the stabilized cycle. In this figure, it is observed that the stabilized cycle loop is almost the same for the swollen B0 and B100. This observation leads to the possibility of excluding the softening effect as the cause of the lowest stress value in swollen B0 rubber. From this perspective, it is important to identify the main driving force for the stretch-stress response obtained from uniaxial fatigue loading. The two possible effects to be considered here are the nature of the swollen rubber due to the effect of diffusion of solvents and the effect from the loading ratio.

3.3. Uniaxial fatigue tests

It was observed that the stress decreases for both dry and swollen rubbers as the number of cycles increases, at all maximum stretch levels imposed. Hence in this paper, we will only present one representative stretch-stress plot for dry and swollen rubbers. Fig. 4a–d show examples of the results at a maximum stretch of 2 for the cycle numbers 10, 100, 1000 and 10,000. The decrease in stress value can be explained by the change of the rubber's stiffness, which falls over long periods of time at a constant maximum stretch and can be attributed to the long-term viscosity and irreversible breakage of polymer chains or crosslinks in the elastomer network [23]. The negative stress values in the graphs indicate that compression occurred during the tests due to stress relaxation. For each number of cycles quoted, the peak stresses are identified and the evolutions of peak stress versus the number of cycles are depicted in Fig. 5d. Here, the solid lines represent the results obtained from the first specimen and the dashed lines represent the second one. A particular zig–zag pattern is observed for the first 10 cycles and this is purely due to the limitation of the machine which is unable to reach the imposed maximum stretch value from the very first cycle. For both dry and swollen rubbers, the stress decreases until it experiences a steep fall which corresponds to the failure of the rubber specimen. Mars [23] was able to identify the stabilized response of the rubber after 128 cycle, where a constant semi-logarithmic rate of stiffness decrease (plateau) was observed from the stress–strain curve under uniaxial fatigue test. This number of cycles was chosen by the author as a baseline to evaluate the load drop in order to determine end of life. As no plateau was observed in our case, such an approach was not applicable.

A mark was drawn onto each curves to illustrate the appearance of a 1 mm crack at its corresponding number of cycles. It is apparent that the 1 mm crack emerged at a number of cycles close to rupture, regardless of the maximum stretch level. This indicates that the crack propagated rapidly after the initiation of a 1 mm crack until it reached complete rupture.

3.4. λ-N curve

As a first approach, maximum stretch was chosen as the predictor for fatigue lifetime. Indeed, the chosen quantity for plotting the Wohler curves has already been widely used [4,24,1]. The maximum stretch was plotted as a function of number of cycles for the appearance of a 1 mm crack and complete rupture as shown in Figs. 6 and 7 respectively. It should be noted that no crack appeared at all for both dry and swollen rubbers at the maximum stretch level of 1.5. Hence, no data was collected for the rubbers in Fig. 6 at the maximum stretch of 1.5. In fact, the end of life of the rubber for this condition was set to be at 2 million cycles even though no occurrence of rupture was observed. Both plots also show the best-fit power-law function to predict the lifetime. In Fig. 7, the end of life of rubber at maximum stretch of 1.5 was not taken into consideration for the power-law fit. Both of these curves clearly exhibit similar trend in which the lifetime of the F-NBR decreased from dry, swollen B0 and was followed by swollen B100. In addition, the swollen rubber behaved similarly to the dry one with respect to the mechanical properties.

3.5. Post-mortem analysis

3.5.1. At the macroscopic scale

An overall feature of the ruptured specimen due to fatigue is illustrated in Fig. 8. A white dashed line was marked on the specimen to illustrate the crack propagation plane. For this case, the crack propagation plane was not perpendicular to the imposed

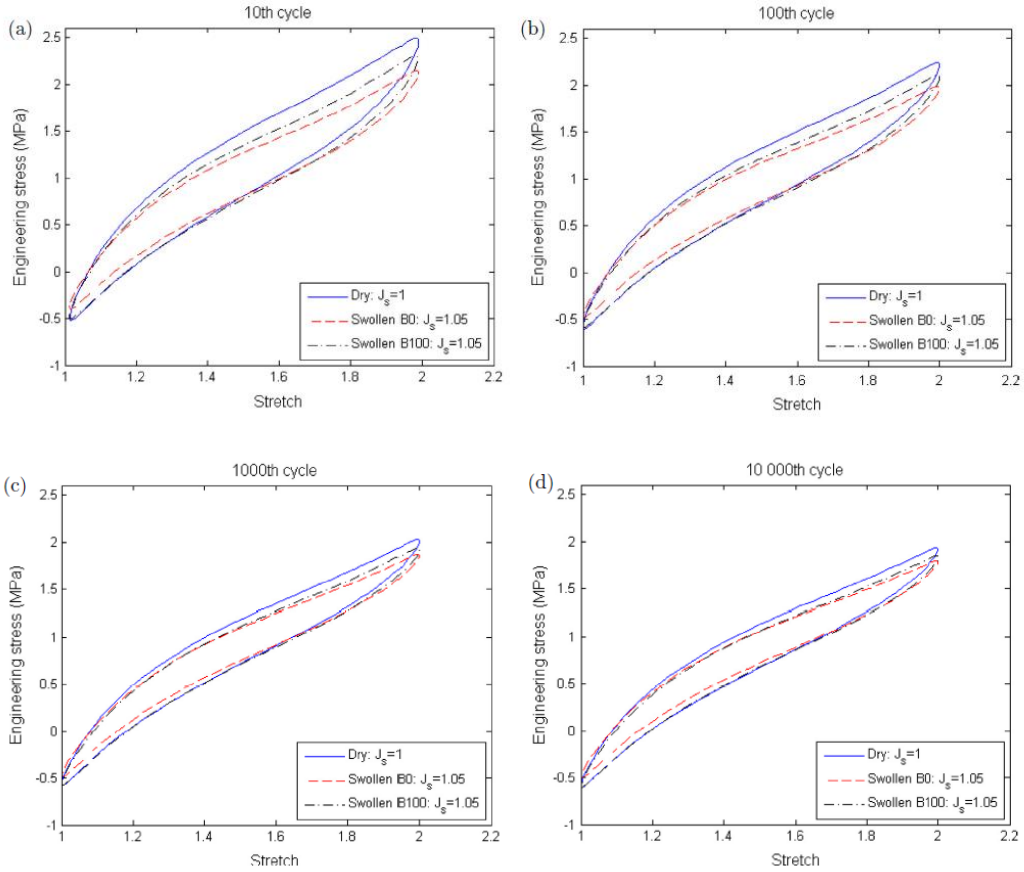

Fig. 4. The stretch-stress responses at different cycles at maximum stretch of 2 under fatigue loading. (a) The stretch-stress responses for cycle number 10 at maximum stretch of 2 under fatigue loading. (b) The stretch-stress responses for cycle number 100 at maximum stretch of 2 under fatigue loading. (c) The stretch-stress responses for cycle number 1000 at maximum stretch of 2 under fatigue loading. (d) The stretch-stress responses for cycle number 10,000 at maximum stretch of 2 under fatigue loading.

uniaxial loading. This was not expected in such non-crystallisable rubbers (see the reported work of Le Cam et al. [19]). It seems to indicate that the hollow geometry had an effect on the mechanical field at the local scale and especially in the crack tip vicinity. Moreover, crack initiation at the macroscopic scale was observed at the specimen surface. Further investigations have been carried out at the microscopic scale in order to define the precise location of crack initiation.

3.5.2. At the microscopic scale

Once the specimens failed, each of the fracture surfaces was observed by FESEM in order to define the crack initiation location, the origin of crack initiation and the specificities of the morphology of the crack propagation zone. Table 5 summarizes the main features observed at different loading conditions for both dry and swollen rubbers: the presence of smooth and rough surfaces, presence of clouded wool, crack initiation location and rubber balling. Rubber balling is one of the fatigue features previously observed in filled natural rubber [6] and short glass fibre–rubber composites [28]. This section divides the achieved results into two categories, which are dry and swollen rubbers, to have a detailed description on the different features reported in the table. The following paragraphs describe the results obtained for dry and swollen rubbers.

(a) Dry rubber.

Fig. 9 shows an example of the fracture surface of dry rubber at microscale with the crack initiating at the specimen surface (see the zones indicated by the dotted lines). It can be deduced that the loading had no effect on the crack initiation zone since it appeared consistently on the surface of rubber for all observed fracture surfaces. To the best knowledge of the authors, no investigations on the fracture surface of nitrile rubber has yet been reported. Hence, our results can not be correlated to other research works on nitrile rubber. Nonetheless, these results can be compared to existing works such as those reported in natural rubber [18] or in styrene-butadiene rubber [19] where the crack initiation occurred from defects located in the subsurface. It has been reported in the literature that the different sources of defects such as carbon black agglomerate failure, cavities at their poles and